Enhancing Subspace-Based Inversions through an Efficient Multi-Scaling Scheme

***Giacomo Oliveri*[1], *Yu Zhong*[2], *Xudong Chen*[2], *and Andrea Massa*[1]**

[1]Eledia Research Group@DISI, University of Trento, 38123 Trento, Italy
Phone: +39 0461 882057, Fax: +39 0461 882063
Email: giacomo.oliveri@disi.unint.it, andrea.massa@ing.unitn.it

[2]Department of Electrical and Computer Engineering, National University of Singapore, 117576 Singapore
Phone: +65 6516 2297, Fax: +65 6779 1103
E-mail: elechenx@nus.edu.sg, yzhong@nus.edu.sg

Abstract

A microwave imaging approach based on the integration of a subspace-base optimization method (*SOM*) and a multi-focusing procedure is proposed. The scattering equations are expressed within the contrast source formulation of the electromagnetic inverse problem and then solved by a nested procedure which includes an outer multi-resolution loop (dealing with the identification of the regions of interest), a spectrum analysis step (devoted to the reconstruction of the 'deterministic' components of the contrast sources) and an inner optimization loop (aimed at the retrieval of their 'ambiguous' parts). A numerical analysis is presented to preliminarily assess the features of the proposed approach.

1. Introduction and Motivation

Electromagnetic inverse scattering problems arise in many applications such as radar imaging, non-destructive testing and evaluation, biomedical diagnostics, remote sensing, subsurface inspection, and material characterization [1-5], and several stochastic [1] and deterministic [6,7] techniques has been developed in the last years for their solution.

In this framework, deterministic techniques based on the contrast source (*CS*) formulation of the inverse scattering problem have received much attention recently [6,7]. Indeed, thanks to the linearity of the "*data*" equation, higher reconstruction accuracies and robustness with respect to the "contrast field" (*CF*) formulation have been obtained [6,7]. However, a limitation of *CS*-methods lies in the non-uniqueness of the associated inverse source problem [8], which is due to the *non-radiating* (or *non-measurable*) components of the unknown contrast source [8].

To overcome this drawback, algorithms which retrieve the *minimum norm* currents and then refine the non-measurable contrast-source components have been proposed [8,9]. In this framework, a subspace optimization method (*SOM*) has been recently introduced [10,11]. In this approach, the contrast source is subdivided in "deterministic" and "ambiguous" parts [10]. Then, the deterministic currents are computed by the spectrum analysis, whereas the ambiguous ones are determined by minimizing a cost functional including both "data" and "state" terms [10].

The *SOM* method has been shown to share several merits of *CSI*-based inversion techniques, while also allowing faster convergences [10]. However, such an approach presents also some limitations. More specifically, it can yield to poor performances if several 'local minima' are at hand, since it is based on a *CG* minimization [10]. Moreover, as the method requires the computation of the singular value decomposition (*SVD*) of the discretized Green operator, computationally expensive inversions can arise especially when dealing with several unknowns [10]. Furthermore, the choice of the *SVD* truncation factor can become critical if no information on the signal-to-noise ratio (*SNR*) is at hand [10].

To overcome these limitations, a new microwave imaging approach based on the integration of a multi-focusing strategy, namely the iterative multi-scaling approach (*IMSA*) [12-14], with the *SOM* method [10] is proposed. After having mathematically formulated the problem at hand (Sect. 2), the proposed *IMSA*−*SOM* method is briefly introduced in Sect. 3, and a preliminary numerical validation is presented (Sect. 4) to assess the potentialities of this approach in comparison with state-of-the-art *SOM* methods.

2. Mathematical formulation

Let us consider a two dimensional inverse scattering problem (z is the longitudinal direction) under transverse magnetic (TM_z) incidence. In a lossless background with permittivity ε_0, a cylindrical scatterer of arbitrary cross section is

978-1-4244-6051-9/11/$26.00 ©2011 IEEE

successively irradiated by V known monochromatic waves $E_{inc}^{v}(\mathbf{r})\hat{z}$, v=1,...,V (whose time dependency factor $exp(j\omega t)$ is omitted). For each incidence v the scattered field $E_{scatt}^{v}(\mathbf{r})\hat{z} = E_{tot}^{v}(\mathbf{r})\hat{z} - E_{inc}^{v}(\mathbf{r})\hat{z}$ is sampled at M measurement points lying in an observation domain D_o (i.e., $\mathbf{r}_m \in D_o$, m = 1,.., M) external to the investigation domain D. According to the *CS* formulation, the following 'data' equation holds true [10]

$$E_{scatt}^{v}(\mathbf{r}_m) = k_0^2 \int_D J^v(\mathbf{r}')G(\mathbf{r}_m/\mathbf{r}')d\mathbf{r}' \qquad \mathbf{r}_m \in D_o, v = 1,...,V, m = 1,...,M \tag{1}$$

where k_0 is the free space wavenumber, $J^v(\mathbf{r}) = \tau(\mathbf{r})E_{tot}^{v}(\mathbf{r})$ is the *contrast source*, $E_{tot}^{v}(\mathbf{r})$ is the total field, $G(\mathbf{r}/\mathbf{r}')$ is the 2*D* free-space Green's function, $\tau(\mathbf{r}) = [\varepsilon(\mathbf{r}) - j\sigma(\mathbf{r})/\omega\varepsilon_0]$ the object function describing the material properties of the nonmagnetic scatterer (assumed constant with respect to z), and $\varepsilon(\mathbf{r})$ and $\sigma(\mathbf{r})$ indicate, respectively, the relative dielectric permittivity and electric conductivity inside the scatterer [10]. Moreover, the following 'state' equation holds true in the investigation domain [10]

$$\tau(\mathbf{r})E_{inc}^{v}(\mathbf{r}) = J^v(\mathbf{r}) - k_0^2\tau(\mathbf{r})\int_D J^v(\mathbf{r}')G(\mathbf{r}/\mathbf{r}')d\mathbf{r}' \quad \mathbf{r} \in D, v = 1,...,V \tag{2}$$

The objective of *CS*-based inverse scattering techniques is to deduce $\tau(\mathbf{r})$, $J^v(\mathbf{r})$ and $E_{tot}^{v}(\mathbf{r})$ in D from the knowledge of $E_{inc}^{v}(\mathbf{r})$ (v=1,…,V, $\forall\mathbf{r}$) and of $E_{scatt}^{v}(\mathbf{r}_m)$ (m=1,...,M, v=1, ...,V).

3. Multi-Scaling Subspace Optimization Method

Inn order to solve (1) and (2), an *IMSA-SOM* method is introduced which is based on the nesting of (*a*) an external *IMSA* loop, whose objective is to correctly locate the regions of interest (*RoI*s) in the investigation domain [12], (*b*) a truncated *SVD* step, aimed at computing the "deterministic" currents in the *RoI*s [10], and (*c*) a *CG*-based iterative optimization step, devoted to find the ambiguous currents [10]. More specifically, the following procedure is proposed:

1. **Problem definition** - define D, M, V. For each view v=1,...,V , collect the scattered field at the M measurement points $\mathbf{E}_{scatt}^{v} = [E_{scatt}^{v}(\mathbf{r}_1),..., E_{scatt}^{v}(\mathbf{r}_M)]$;
2. **Initialization** - set s = 1. Define a (coarse) N-sized grid $\mathbf{r}_n^{(s=1)} = [r_1^{(s=1)},..., r_N^{(s=1)}]$ to discretize Eqs. (1) and (2) according to a coupled dipole method (*CDM*) [10];
3. **Matrix computation** - Evaluate the samples of the incident field $\mathbf{E}_{inc}^{v}\Big|^{(s)} = [E_{inc}^{v}(r_1^s),..., E_{inc}^{v}(r_N^s)]$. Compute the Green matrices $H^{(s)}$ and $G^{(s)}$ according to

$$H^{(s)} = \begin{bmatrix} g(\mathbf{r}_1^{(s)}, \mathbf{r}_1^{(s)}) & \cdots & g(\mathbf{r}_1^{(s)}, \mathbf{r}_N^{(s)}) \\ \vdots & \ddots & \vdots \\ g(\mathbf{r}_N^{(s)}, \mathbf{r}_1^{(s)}) & \cdots & g(\mathbf{r}_N^{(s)}, \mathbf{r}_N^{(s)}) \end{bmatrix} \tag{3}$$

$$G^{(s)} = \begin{bmatrix} g(\mathbf{r}_1^{(s)}, \mathbf{r}_1^{(s)}) & \cdots & g(\mathbf{r}_1^{(s)}, \mathbf{r}_N^{(s)}) \\ \vdots & \ddots & \vdots \\ g(\mathbf{r}_M^{(s)}, \mathbf{r}_1^{(s)}) & \cdots & g(\mathbf{r}_M^{(s)}, \mathbf{r}_N^{(s)}) \end{bmatrix} \tag{4}$$

   where $g(\mathbf{r}_p^{(s)}, \mathbf{r}_q^{(s)})$ is the discretized Green operator [10];
4. **Estimation of deterministic currents** - Compute the *SVD* of $G^{(s)}=U^{(s)}X^{(s)}(V^{(s)})^T$ (^{T} being the transpose operator), select the 'truncation factor' $L^{(s)}$ [10] and deduce the deterministic part of the contrast source $\mathbf{I}_{\det}^{v}\Big|^{(s)}$ according to

$$\mathbf{I}_{\det}^{v}\Big|^{(s)} = V_{\det}^{(s)}\left(X_{\det}^{(s)}\right)^{-1}\left(U_{\det}^{(s)}\right)^T \mathrm{E}_{scatt}^{v} \tag{5}$$

   where the subscript *det* identifies the truncated versions of the matrices at the $L^{(s)}$-th singular value [10];
5. **Iterative estimation of ambiguous currents and contrast** – Minimize by $T^{(s)}$ iterations of a *CG* method the cost function

$$F^{(s)} = \sum_{v=1}^{V}\left(\Delta_{data}^{v}\Big|^{(s)} \Big/ \left\|\mathbf{E}_{scatt}^{v}\right\|^2 + \Delta_{state}^{v}\Big|^{(s)} \Big/ \left\|\mathbf{I}_{\det}^{v}\Big|^{(s)}\right\|^2\right) \tag{6}$$

where $\Delta^{v}_{data}\Big|^{(s)}$ and $\Delta^{v}_{state}\Big|^{(s)}$ are the v-th view 'data' and 'state' *misfits* at the current *IMSA* step [computed by the discretized versions of (1) and (2)], respectively. Then evaluate the retrieved ambiguous currents and contrast from

$$\mathbf{I}^{v}_{amb}\Big|^{(s)} = V^{(s)}_{amb}\,\mathbf{a}^{v}_{opt}\Big|^{(s)} \tag{7}$$

$$\tau\left(\mathbf{r}^{(s)}_{n}\right) = \frac{j\eta_0}{k_0 A\left(D^{(s)}_{n}\right)}\left\{\sum_{v=1}^{V}\left[\left[E^{v}_{tot}\left(\mathbf{r}^{(s)}_{n}\right)\Big|_{opt}\right]^{*}\left[I^{v}\left(\mathbf{r}^{(s)}_{n}\right)\Big|_{opt}\right]\Big/\left\|\mathbf{I}^{v}_{\det}\Big|^{(s)}\right\|^{2}\right]\right\}\Bigg/\left\{\sum_{v=1}^{V}\left[\left\|E^{v}_{tot}\left(\mathbf{r}^{(s)}_{n}\right)\Big|_{opt}\right\|^{2}\Big/\left\|\mathbf{I}^{v}_{\det}\Big|^{(s)}\right\|^{2}\right]\right\} \tag{8}$$

where $A\left(D^{(s)}_{n}\right)$ is the n-th cell area, η_0 is the free-space impedance, and $\mathbf{a}^{v}_{opt}\Big|^{(s)}$, $I^{v}\left(\mathbf{r}^{(s)}_{n}\right)\Big|_{opt}$, and $E^{v}_{tot}\left(\mathbf{r}^{(s)}_{n}\right)\Big|_{opt}$ are the estimated ambiguous current, contrast source, and total field and at the $T^{(s)}$-th *CG* step [10];

6. **Identification of** *RoI***s** - Filter and cluster the retrieved profile $\tau\left(\mathbf{r}^{(s)}_{n}\right)$ to identify the regions of interest [12];
7. **Convergence check** - If a "stationary condition" [12] on the *RoI*s is satisfied or $s = S$, terminate. Otherwise, set s=s+1, define a locally refined grid $\mathbf{r}^{(s)}_{n}$ (n=1,...,N) to discretize the *RoI*s, and goto 3.

4. Preliminary Numerical Assessment

A preliminary numerical analysis is presented in this section to assess the features of the proposed *IMSA−SOM* method with respect to state-of-the-art *SOM* approaches. Towards this end, an investigation domain of size $2.4\lambda\times2.4\lambda$ (free-space background) is illuminated by V=24 *TM* plane waves. The total field is calculated through a *MoM*-based solver and an *AWG* noise (SNR=10 dB) is added to the its samples collected at M=24 measurement points (located on a circle of radius 1.8λ). In all the inversion procedures, $T^{(s)}$=100 and $L^{(s)}$ has been selected so that the 90% most significant singular values of the $G^{(s)}$ spectrum are included in the 'deterministic' current computation [Eq. (5)]. Moreover, the maximum number of IMSA steps has been set to S=4.

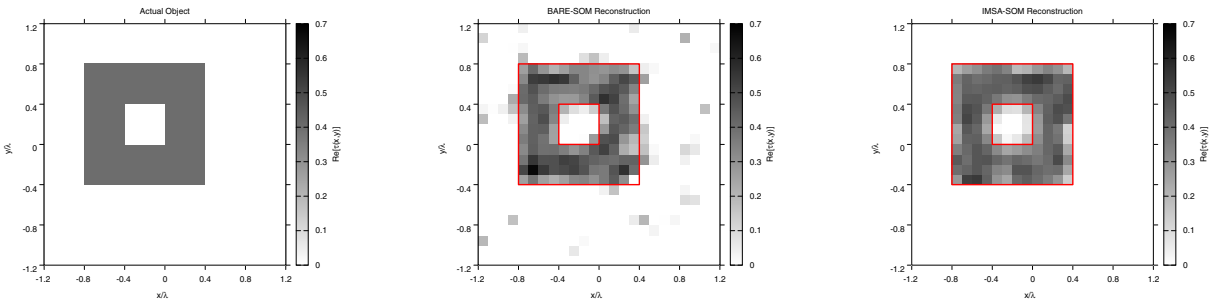

(*a*) (*b*) (*c*)

Figure 1. [*Hollow Cylinder*, $\tau = 0.4$, *SNR*=10 dB] Actual (*a*) and retrieved τ by (*b*) *BARE-SOM* and (*c*) *IMSA-SOM*.

In the first numerical example, a lossless hollow scatterer with $\tau = 0.4$ is considered [Fig. 1(*a*)]. The plots of the retrieved dielectric profiles by a standard *SOM* method [*BARE-SOM* - Fig. 1(*a*)] and by the *IMSA-SOM* approach [Fig. 1(*c*)] indicates that although both methods are able to identify the presence of a single hollow scatterer, the multi-focusing method yields to an higher accuracy in terms of retrieved contrast. Moreover, thanks to its zooming procedure, the *IMSA-SOM* completely avoids artifacts outside the object support, unlike the *BARE-SOM* [Fig. 1(*b*) vs. 1(*c*)].

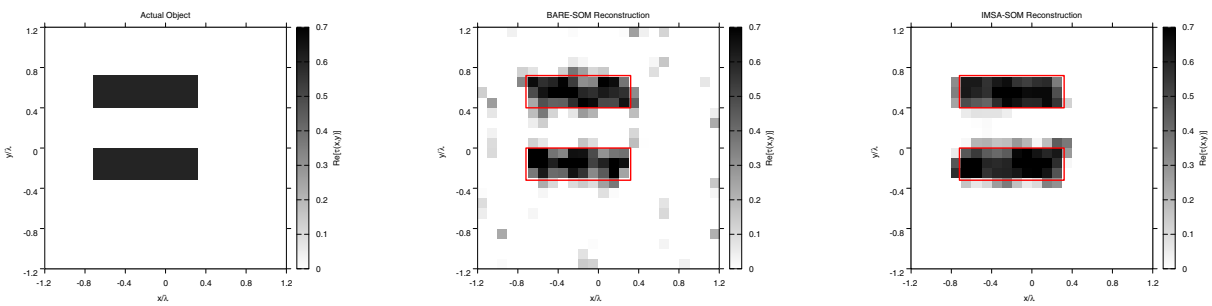

(*a*) (*b*) (*c*)

Figure 2. [*Parallel Cylinders*, $\tau = 0.6$, *SNR*=10 dB] Actual (*a*) and retrieved τ by (*b*) *BARE-SOM* and (*c*) *IMSA-SOM*.

Similar conclusions hold true also when dealing with multiple scatterers. Indeed, the next numerical experiment, concerned with two parallel cylinders with $\tau = 0.6$ [Fig. 2(*a*)], confirms that the *IMSA-SOM* is able to correctly retrieve the position, shape and permittivity of the inspected objects, while the *BARE* methodology yields to a lower accuracy. It is also worth remarking that, despite the exploitation of a single-region focusing methodology, the two objects are correctly separated by the *IMSA* method. Moreover, a multi-region version of the *IMSA-SOM* approach able to efficiently deal with multiple distant objects is at present under development.

5. Conclusion

The integration of a multi-focusing procedure and a subspace-base optimization method (*SOM*) is introduced within the contrast source formulation of the electromagnetic inverse problem. A nested procedure is implemented for the solution of the arising inverse problem. The presented preliminary numerical validation has shown the effectiveness and accuracy of the method in comparison with a state-of-the-art *SOM* approach.

6. References

1. P. Rocca, M. Benedetti, M. Donelli, D. Franceschini, and A. Massa, "Evolutionary optimization as applied to inverse scattering problems", *Inverse Problems*, vol. 25, no 6, pp. 1-41, art. no. 123003, Dec. 2009.

2. R. Zoughi, *Microwave Nondestructive Testing and Evaluation*, Amsterdam, The Netherlands: Kluwer, 2000.

3. P. M. Meaney, M. W. Fanning, D. Li, S. P. Poplack, and K. D. Paulsen, "A clinical prototype for active microwave imaging of the breast," *IEEE Trans. Microw. Theory Tech.*, vol. 48, pp. 1841-1853, Nov. 2000.

4. S. Caorsi, A. Massa, and M. Pastorino, "A computational technique based on a real-coded genetic algorithm for microwave imaging purposes," *IEEE Trans. Geosci. Remote Sens*., vol. 38, no. 4, pp. 1697-1708, Jul. 2000.

5. M. Donelli and A. Massa, "A computational approach based on a particle swarm optimizer for microwave imaging of two-dimensional dielectric scatterers," *IEEE Trans. Microwave Theory Tech*., vol. 53, no. 5, pp. 1761-1776, May 2005.

6. P. M. van den Berg and R. E. Kleinman, "A contrast source inversion method," *Inv. Probl.*, vol. 13, no. 6, pp. 1607-1620, Dec. 1997.

7. P. M. van den Berg and A. Abubakar, "Contrast source inversion method: State of art," *Progress Electromagn. Res.*, vol. 34, pp. 189–218, 2001.

8. P. Rocca, M. Donelli, G. L. Gragnani, and A. Massa, "Iterative multi-resolution retrieval of non-measurable equivalent currents for the imaging of dielectric objects," *Inv. Probl*., vol. 25, 055004, pp. 1-15, 2009.

9. T. M. Habashy, M. L. Oristaglio, and A. T. de Hoop, "Simultaneous nonlinear reconstruction of two-dimensional permittivity and conductivity," *Radio Sci.*, vol. 29, no. 4, pp. 1101-1118, Jul. 1994.

10. X. Chen, "Subspace-based optimization method for solving inverse-scattering problems", *IEEE Trans. Geosci. Remote Sens.*, vol. 48, no. 1, pp. 42-49, Jan. 2010.

11. Y. Zhong, X, Chen, and K. Agarwal, "An improved subspace-based optimization method and its implementation in solving three-dimensional inverse problems," *IEEE Trans. Geosci. Remote Sens.*, vol. 48, no. 10, pp. 3763-3768, Oct. 2010.

12. S. Caorsi, M. Donelli, D. Franceschini, and A. Massa, "A new methodology based on an iterative multiscaling for microwave imaging," *IEEE Trans. Microwave Theory Tech.*, vol. 51, no. 4, pp. 1162-1173, Apr. 2003.

13. S. Caorsi, M. Donelli, and A. Massa, "Detection, location, and imaging of multiple scatterers by means of the iterative multiscaling method," *IEEE Trans. Microwave Theory Tech.*, vol. 52, pp. 1217-1228, Apr. 2004.

14. M. Donelli, G. Franceschini, A. Martini, and A. Massa, "An integrated multiscaling strategy based on a particle swarm algorithm for inverse scattering problems," *IEEE Trans. Geosc. Remote Sens*., vol. 44, no. 2, pp. 298-312, Feb. 2006.